Polypropylene/Layered Double Hydroxide (LDH) Nanocomposites: Influence of LDH Particle Size on the Crystallization Behavior of Polypropylene[†]

Baku Nagendra,[‡,§] Kiran Mohan,[⊥] and E. Bhoje Gowd*[,‡,§]

[‡]Materials Science and Technology Division, [§]Academy of Scientific and Innovative Research (AcSIR), and [⊥]Chemical Sciences and Technology Division, CSIR-National Institute for Interdisciplinary Science and Technology, Trivandrum, Kerala 695001, India

Ⓢ *Supporting Information*

ABSTRACT: Highly dispersed isotactic polypropylene (iPP) nanocomposites were prepared by incorporating two different sized Mg−Al LDH nanoparticles with different loadings from 1 to 10 wt % using a modified solvent mixing method. Larger sized LDH nanoparticles (∼3−4 μm) were prepared from the gel form of Mg−Al LDH, and the smaller sized nanoparticles (∼50−200 nm) were prepared by sonication of as-synthesized LDH particles. Such obtained LDH nanoparticles were carefully characterized using wide-angle X-ray diffraction (WAXD), transmission electron microscopy, and scanning electron microscopy. WAXD and atomic force microscopy results indicate that the LDH nanoparticles were highly dispersed in the iPP matrix. The influence of LDH nanoparticles size and concentration on the thermal stability, spherulitic morphology, melting behavior, isothermal crystallization kinetics, and lamellar structure of iPP were investigated. Incorporation of low loadings of sonicated LDH particles (e.g., 1−2.5 wt %) show substantial effect on thermal stability, spherulite size, crystallinity, and crystallization half-time and lamellar morphology of iPP compared to the pure iPP and that of nanocomposites with larger LDH particles with same loadings. The better nucleation ability of iPP in the presence of sonicated LDH can be attributed to the high surface area of LDH nanoparticles along with its better dispersibility within the polymer matrix. The incorporation of LDH nanoparticles does not change the crystallization growth mechanism and crystal structure of iPP.

KEYWORDS: nanocomposites, isotactic polypropylene, sonication, solvent blending, thermal stability, crystallization
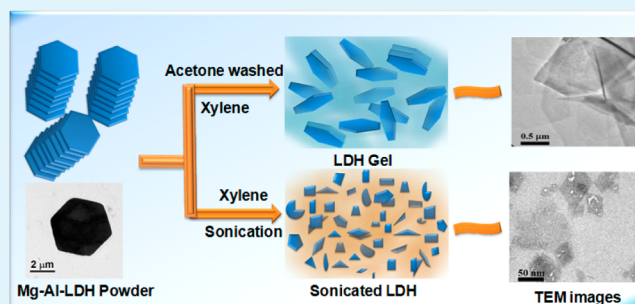
INTRODUCTION

Polymer based nanocomposites filled with nanosized stiff particles have evolved and attracted great interests from both in industry and academia during the last two decades.[1−5] A range of layered materials of varying dimensions have been used as nanofillers, but the most commercial importance is engaged with layered materials such as clays and related phyllosilicates.[2,6,7] Performance of polymer nanocomposites strongly depends on the degree of dispersion and aspect ratio of layered materials in the polymer matrices. In particular, exfoliation of layered materials in polymer matrices has been shown to improve the flame retardancy, optical, thermal, rheological and mechanical properties of base polymer.[1−7] In most cases, layered materials are surface-modified with organic compounds for improving the dispersion in the polymer matrix.

Lately, layered double hydroxides (LDH) are considered as a new emerging class of nanofillers for the preparation of multifunctional polymer/LDH nanocomposites.[1,5,8,9] LDH layers are 0.48−0.49 nm thick, and their lateral dimensions can be varied between few nm and several μm by adjusting the synthetic conditions.[10−13] Important feature of these materials is tremendous flexibility in tuning the composition of both

inorganic layers as well as balancing anions in the interlayer space.[1] Preparation of highly exfoliated polymer nanocomposites using LDH is always a great challenge because of the stronger electrostatic interlayer interactions due to their higher charge density. To date, variety of polymer systems were used in nanocomposites preparation with LDH, which include polyethylene,[14−16] polypropylene,[17−20] polyamides,[21,22] polystyrene,[23] polylactic acid,[24,25] poly(methyl methacrylate),[26] poly(vinyl chloride),[27] etc. In most of these nanocomposites, either the LDH was modified with the organic compounds (surfactants) or the polymer itself was modified to facilitate the miscibility between the hydrophobic polymer and the hydrophilic LDH to achieve intercalated or exfoliated nanocomposites.[1,9,14−20] However, these modifications could lead to additional steps in the preparation of nanocomposites, unwanted change in the polymer characteristics and possible

degradation of organic modifiers upon the processing of these nanocomposites.[14] The end-use applications of polymer nanocomposites would be greatly expanded with surfactant-free materials. Varieties of LDH have been used in the preparation of nanocomposites with polymers, which include Co−Al LDH,[19] Mg−Al LDH,[17,18] Zn−Al LDH,[16,28] etc. In the present study, Mg−Al LDH was chosen because of its white color and its resemblance to the commonly used fire retardant metal hydroxides.

Few reports are available in the literature to demonstrate the exfoliation of the LDH and the preparation of exfoliated polymer/LDH nanocomposites using surfactant-free LDH.[18,28−30] The pioneering group of Dermot O'Hare has reported an aqueous miscible organic solvent treatment (AMOST) method for the preparation of stable dispersions of surfactant free LDH in nonpolar solvents and the subsequent preparation of exfoliated polypropylene/LDH nanocomposites (PP) by solution mixing.[18,28,31] The advantage of the AMOST method is the conversion of the hydrophilic LDH layers to hydrophobic, so that the miscibility can be achieved between the LDH and hydrophobic polymer.

In semicrystalline polymer nanocomposites, the dispersed nanofillers can induce the structural and morphological changes of the polymer matrix and therefore control the various properties of the nanocomposites. The study on crystallization of polymer nanocomposites is of great technical importance, in view of the fact that the nanofillers alter the crystallization behavior and the extent of crystallinity that in turn depends on the processing conditions. A number of studies were aimed to elucidate the influence of nanosized filler on the crystallization behavior of semicrystalline polymers.[3,32,33] Isotactic polypropylene (iPP) is one of those most widely used thermoplastic polymers in the polymer industry because of its easy processability and good balance between properties and cost. In spite of extensive studies on the crystallization behavior of iPP in the presence of various nanofillers such as layered silicates,[34,35] carbon nanotubes,[36,37] and graphene,[38] limited attention has been given to iPP/LDH nanocomposites. Lonkar et al. studied the crystallization behavior of iPP in the presence of organically modified LDH and found that LDH could alter the type of nucleation, growth, and geometry of PP crystals.[20,39] However, to our knowledge, no studies have been conducted on the crystallization behavior of iPP in the presence of unmodified LDH.

In the present study, we prepared iPP/Mg−Al LDH nanocomposites by two different methods using unmodified LDH. In the first method, the gel form of Mg−Al LDH was directly dispersed in iPP solution to prepare highly dispersed nanocomposites. In another method, for the first time, sonicated LDH was used for the preparation of highly dispersed nanocomposites. Sonication of LDH for longer duration leads to the formation of hydrophobic surfaces, which enable them to be highly dispersible in nonpolar polymer solutions. This study also aims at unravelling the influence of unmodified LDH and its particle size on the crystallization behavior of iPP using differential scanning calorimetry and polarized optical microscopy. It was found that, iPP/LDH nanocomposites containing smaller sized LDH nanoparticles (∼50−200 nm) showed better thermal stability and nucleation ability compared to that of iPP/LDH nanocomposites containing larger sized LDH nanoparticles (∼3−4 μm) with the same loading.

■ EXPERIMENTAL SECTION

Synthesis of Mg−Al LDH. Synthesis of Mg−Al LDH was carried out in a two-neck round-bottom flask equipped with a reflux condenser under the ambient atmospheric conditions by the coprecipitation method. Magnesium nitrate $(Mg(NO_3)_2 \cdot 6H_2O)$, aluminum nitrate $(Al(NO_3)_3 \cdot 9H_2O)$, and urea were dissolved in Millipore water in the ratio 2:1:7 to give the final concentrations of 10, 5, and 35 mM, respectively. Then, the mixture was refluxed at 100 °C under continuous stirring for 24 h. Finally, the precipitate was washed with hot Millipore water to remove the unreacted reactants if any and vacuum-dried at 60 °C for 24 h. Similarly, the experiment was repeated in argon (Ar) atmosphere to verify the influence of the reaction environment on the morphology of LDH (data not shown here).

LDH Gel Preparation. Vacuum dried Mg−Al LDH was redispersed in acetone and stirred the dispersion at ambient temperature for 1 h. Then the precipitate was filtered and repeatedly washed with acetone. Such obtained LDH powder was dispersed in xylene and stirred it for 12 h at ambient temperature. The resulting colloidal suspension was stable at room temperature for few minutes and after that LDH slowly settled down as sediment. Decanting of the excess xylene leads to the formation of a transparent gel (Figure S1).

Sonication of LDH. As prepared LDH dry powder was dispersed in xylene and sonicated for 4 days using an ultrasonic sonication bath at room temperature. Enough care was taken to avoid the temperature increase during sonication. The resulting suspension was stable at room temperature for a few hours.

Preparation of Polypropylene/LDH Nanocomposites. Isotactic polypropylene used in this study had a weight-average of 120 000 g/mol with a polydispersity index of 4.5. The nanocomposites of iPP/Mg−Al LDH were prepared by two different routes using solution blending method. In one case, nanocomposites of iPP/Mg−Al LDH with different compositions (0, 2.5, and 5% LDH) were obtained using the gel form of LDH. In this case, 10 g of iPP was dissolved in 100 mL of xylene in a round-bottom flask at 150 °C with continuous stirring under argon atmosphere. After the complete dissolution of iPP, the required amount of Mg−Al LDH xylene gel was added to the flask under continuous stirring. In another case, the dispersion of LDH in xylene was prepared by sonication of required amount of LDH for 4 days. Such sonicated LDH dispersion was added to the required amount of iPP solution in a round-bottom flask at 150 °C with continuous stirring under argon atmosphere. The amount of LDH was adjusted to different weight percent to prepare nanocomposites with different LDH contents (0, 1, 2.5, 5, and 10% LDH). The resultant solution was refluxed at 150 °C for 24 h for the homogeneous dispersion of LDH platelets in iPP solution. The polymer solution was poured into 100 mL of ethanol. The precipitate was filtered, washed with ethanol several times, and dried in a vacuum oven at 100 °C for 24 h.

■ CHARACTERIZATION

Wide- and Small-Angle X-ray Scattering (WAXS/SAXS). WAXS/SAXS measurements were carried out on XEUSS SAXS/WAXS system using a Genix microsource from Xenocs operated at 50 kV and 0.6 mA. The Cu Kα radiation (λ = 1.54 Å) was collimated with FOX2D mirror and two pairs of scatter less slits from Xenocs. The 2D-patterns were recorded on a Mar345 image plate and processed using Fit2D software. All the measurements were made in the transmission mode. The sample to detector distance, which was calibrated with silver behenate standard, was 1044 mm for SAXS and 214.5 mm for WAXS, respectively. All the samples were crystallized under controlled conditions to understand the effect of LDH on the crystallization behavior of iPP. Samples were melted at 200 °C in DSC for approximately 5 min to remove the previous thermal history and are rapidly quenched to the isothermal crystallization temperature (130 °C). Samples were allowed to

crystallize at 130 °C for 1 h (Figure S2). Such prepared samples were used for SAXS and WAXS analysis.

Surface Area Analysis. The specific surface area was measured using the Brunauer, Emmet, and Teller (BET) surface area analyzer (Micrometrics TriStar 3000 V6.05A). Surface areas were measured from the Nitrogen adsorption using the multipoint method after degassing the LDH powders at 150 °C for 2 h.

Fourier Transform Infrared Spectroscopy (FTIR). The infrared spectra were measured with a PerkinElmer series FT-IR spectrometer-2 over the wavenumber range of 4000−400 cm^{-1}. The powder sample was mixed with KBr and pressed in the form of pellets. The FTIR spectra were collected with 32 scans and a resolution of 1 cm^{-1}.

Scanning Electron Microscopy (SEM). Surface morphology of the LDH was investigated using SEM (Zeiss EVO 18 cryo SEM) with an accelerating voltage of 20 kV. LDH suspensions in water were deposited over a glass coverslip, which is pasted onto a carbon-coated grid and imaged after natural drying at room temperature.

Transmission Electron Microscopy (TEM). TEM images were recorded on a JEOL 2010 transmission electron microscope operating at 300 kV. As-prepared LDH particles were dispersed in water and directly deposited on a carbon-coated copper grid. In another case, after acetone treatment/sonication, LDH samples were dispersed in xylene and deposited on a carbon-coated copper grid. All the grids were dried for 2 days and imaged under transmission electron microscope. The elemental constitution of the materials was determined on an energy dispersive spectrometer (Technai G^2 30LaB$_6$, ST with EDS).

Thermogravimetric Analysis (TGA). The TGA thermograms were recorded in the heating process by using thermo gravimetric analysis TA Q50 under nitrogen gas atmosphere at a rate of 10 °C/min.

Differential Scanning Calorimetry (DSC). The crystallization and melting behavior of all samples were measured using a differential scanning calorimeter (PerkinElmer Pyris 6 DSC). The melt crystallization temperature (T_{mc}) was measured for iPP and iPP/LDH nanocomposites. In this case, the sample was first heated from room temperature to 200 °C (above melting temperature of iPP) at a rate of 10 °C/min, where it was held for 1 min to erase the thermal history of the sample, then cooled at a rate of 10 °C/min to room temperature to measure the T_{mc}. All the samples were reheated to 200 °C to measure the melting temperature. In another set of experiments, the crystallization half-time was measured at isothermal crystallization temperature. The thermal program employed for the isothermal crystallization is depicted in Figure S2. Molten samples were rapidly cooled to a desired crystallization temperature (T_c) i.e. 130 °C at a rate of 100 °C/min and kept for 60 min for the isothermal crystallization. All the DSC experiments were conducted under a nitrogen atmosphere.

Polarized Optical Microscopy (POM). A polarized optical microscope (Universal polarizing microscope ZPU01, Carl Zeiss Inc.) equipped with a Linkam hot stage was used to monitor the spherulites. Average spherulite size was measured manually using ImageJ software. This size corresponds to the average equatorial diameter of the spherulite. The thin-film specimens were prepared by melting the samples at 200 °C for 1 min and then rapidly cooled to the crystallization temperature.

Atomic Force Microscopy (AFM). Atomic force microscopy (Digital Instruments, Inc., Santa Barbara) (AFM) imaging was performed using a Dimension 3100 and a CP microscope (Park Scientific Instrument, Inc.) in the tapping mode.

■ RESULTS AND DISCUSSION

Synthesis and Characterization of Mg−Al LDH. The Mg−Al LDH used in this study was synthesized by coprecipitation method under ambient atmospheric conditions.[40] The powder X-ray diffraction patterns confirmed the formation of LDH structure, exhibiting sharp reflections corresponding to the (00n) planes (Figure 1a). The TEM
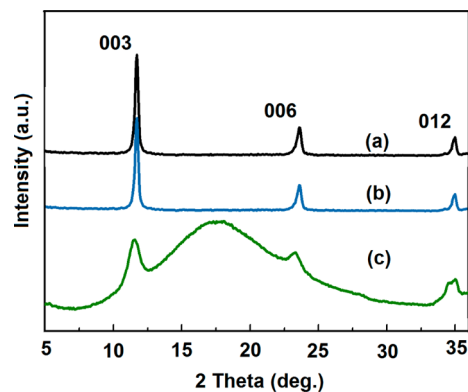
Figure 1. Powder X-ray diffraction patterns of (a) as-prepared Mg−Al LDH, (b) sonicated LDH, and (c) Mg−Al LDH gel.

(Figure 2a) and SEM (Figure 3a and b) images show the stacked hexagonal platelets with a mean lateral size of 3.5 μm. As-prepared LDH platelets had a dark contrast, indicating the presence of several layers of hexagonal platelets in a single particle. The energy-dispersive X-ray spectra (EDS) confirmed the composition of the as-prepared Mg−Al LDH (Figure 2b). The dominant oxygen peak in EDS indicates the presence of water molecules within the layers of the LDH platelets. FTIR spectrum of the Mg−Al LDH also confirmed the presence of CO_3^{2-}, NO_3^{-}, and water molecules (Figure S3). The characteristic band for interlayer carbonate (CO_3^{2-}) and interlayer nitrate (NO_3^{-}) were observed at 1356 and 1382 cm^{-1}, respectively. Urea, which was used as base to prepare LDH, readily undergoes hydrolysis in the presence of water at 100 °C to give ammonium carbonate. Such obtained ammonium carbonate further converted into ammonia and carbonate to hydrogen carbonate.[41] These conditions favored the formation of CO_3^{2-} along with the NO_3^{-}. The broad band at 3444 cm^{-1} is due to the O−H stretching of the metal hydroxide layer and interlayer H$_2$O molecules. Another band centered at 1607 cm^{-1} is assigned to be the interlayer water (H$_2$O) molecule.

Swelling and Exfoliation of Mg−Al LDH. O'Hare and co-workers reported that treatment of as-prepared LDH by aqueous miscible organic solvent converts the hydrophilic LDH to hydrophobic.[18] Herein, we adopted their method to prepare the dispersions of LDH in nonpolar solvents like xylene. Further storage of such dispersion resulted in a transparent gel-like aggregate (Figure S1). Figure 1c shows the powder X-ray pattern of gel-like aggregate. The 00n reflections are somewhat broad and low in intensity, which may be due to stacking disorder of LDH platelets in the swollen state. A broad amorphous-like halo was also observed at $2\theta \sim 17.5°$ due to the
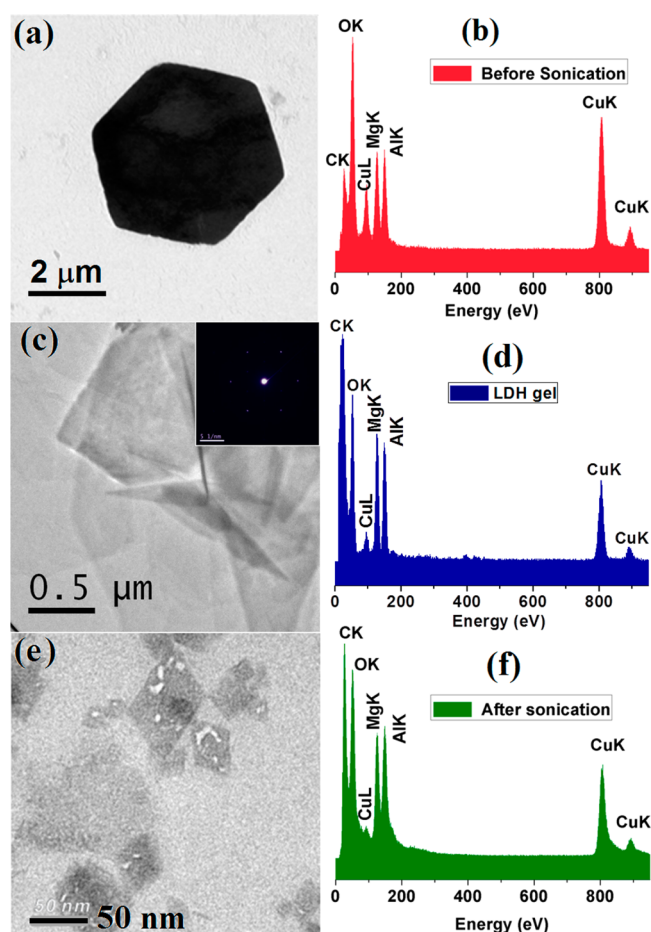
Figure 2. TEM images of (a and b) as-prepared Mg−Al LDH and corresponding EDS spectrum, (c and d) delaminated Mg−Al LDH and corresponding EDS spectrum (inset) selected area electron diffraction (SAED) pattern of delaminated Mg−Al LDH, (e and f) sonicated LDH and corresponding EDS spectrum.

scattering of xylene. It is also important to mention here that X-ray measurements of gels were made in the open capillaries, where there was a possibility for solvent evaporation during the X-ray measurement. TEM image of Mg−Al LDH gel dispersed in xylene clearly showed the delamination of LDH platelets to single-layer nanosheets (Figure 2c). Due to the thin nature of exfoliated single-layer nanosheets, contrast of the single-layer is very weak. The selected area electron diffraction (SAED) (inset of Figure 2c) shows hexagonally arranged spots, indicating that the delaminated nanosheets are single crystalline.[40] The corresponding EDS (Figure 2d) shows the drastic reduction in the oxygen peak compared to their bulk LDH structure, indicating the removal of interlayer H_2O molecules from the

stacked structure. The surface area measured for LDH gel (after drying) was 200 ± 5 m^2/g. Liquid exfoliation of LDH is known for quite some time, and it has emerged as a process in producing the novel two-dimensional materials.[29,42,43] Wu et al. demonstrated the gel formation in LDH−NO$_3$ in formamide without incorporation of surfactants.[44] However, their procedure did not work for carbonate containing LDH as carbonate is a much stronger hydrotalcite-builder than nitrate. Very recently, Song et al. used an anion exchange process to increase the interlayer spacing and subsequently delaminated the bulk LDH to single-layer nanosheets.[29] In the present study, by taking advantage of the AMOST method, we successfully exfoliated the bulk Mg−Al LDH to single-layer nanosheets.

Sonication of Mg−Al LDH. Ultrasonic vibration (sonication) has been used in the fabrication of two-dimensional nanosheets such as graphene, transition metal oxides, and transition metal dichalcogenides from bulk layered materials in liquid.[43,45,46] In the present study, we used sonication method to prepare stable dispersions of LDH in nonpolar solvents. Figure 1b shows the powder X-ray diffraction pattern of sonicated LDH powder. The sharp reflections corresponding to the (00n) planes indicate the retention of crystal structure upon the sonication. No traces of impurities were observed in sonicated LDH powders. The TEM (Figure 2e) and SEM images (Figure 3c) of the sonicated sample show the broken platelets of LDH layers and the lateral size reduced to few tens of nanometers. The corresponding energy-dispersive X-ray spectrum shown in Figure 2f is consistent with the EDS spectrum of bulk LDH. However, a noteworthy change was observed upon the sonication, i.e., the oxygen peak decreased in intensity drastically indicating the removal of water molecules from bulk LDH. During sonication, water molecules present within the LDH layers are replaced by xylene molecules, weakening the interlayer attraction. Then, further sonication can completely take apart the layers, resulting in an exfoliated dispersion. Simultaneously, the LDH layers are broken into small fragments in the sonication process. The surface area measured for sonicated LDH powder was 710 ± 5 m^2/g. Qiu and co-workers observed the breakage of organically modified Zn−Al LDH platelets in xylene with refluxing time.[47]

Synthesis and Characterization of iPP/Mg−Al LDH Nanocomposites. Figure 4 shows the schematic illustration of the method used for the preparation of highly dispersed iPP nanocomposites by two different methods using Mg−Al LDH. In first method, a transparent gel-like aggregate of Mg−Al LDH was directly added to the iPP solution. Treatment of as-prepared LDH with acetone followed by dispersion in xylene helps in the removal of interlayer H_2O molecules from the stacked LDH structure. The swollen LDH platelets were readily
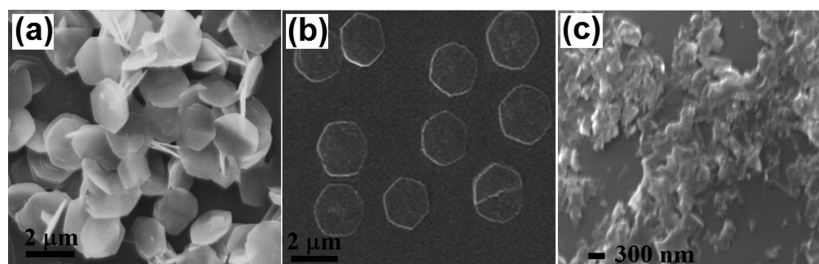
Figure 3. Scanning electron microscope images of (a and b) Mg−Al LDH dispersed in water and (c) sonicated LDH.
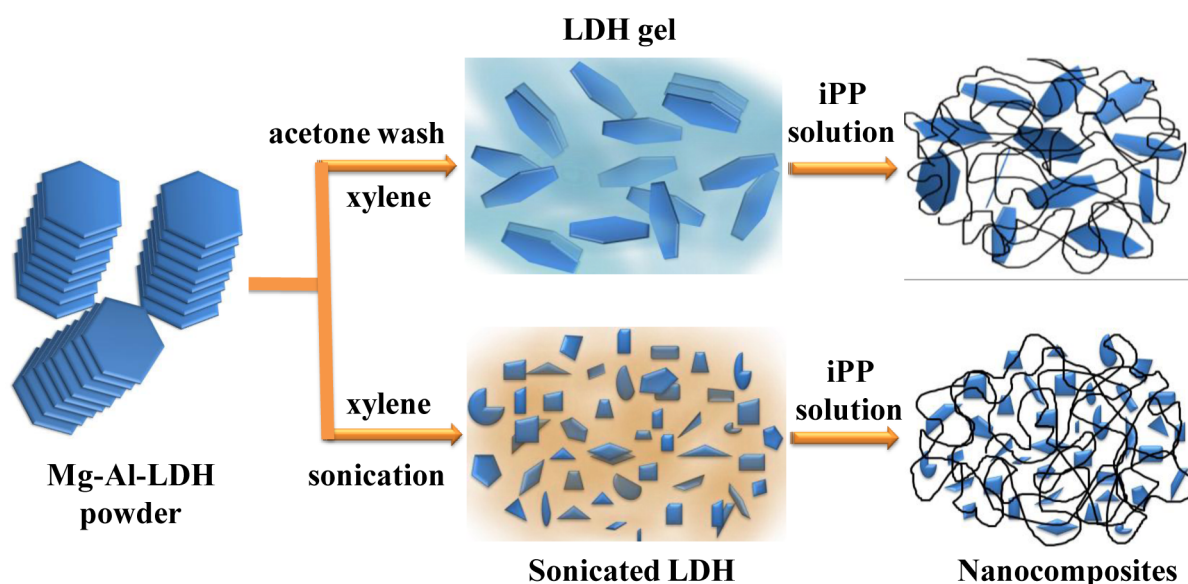
Figure 4. Schematic illustration of the polymer nanocomposite preparation based on isotactic polypropylene and Mg−Al LDH layered double hydroxide.
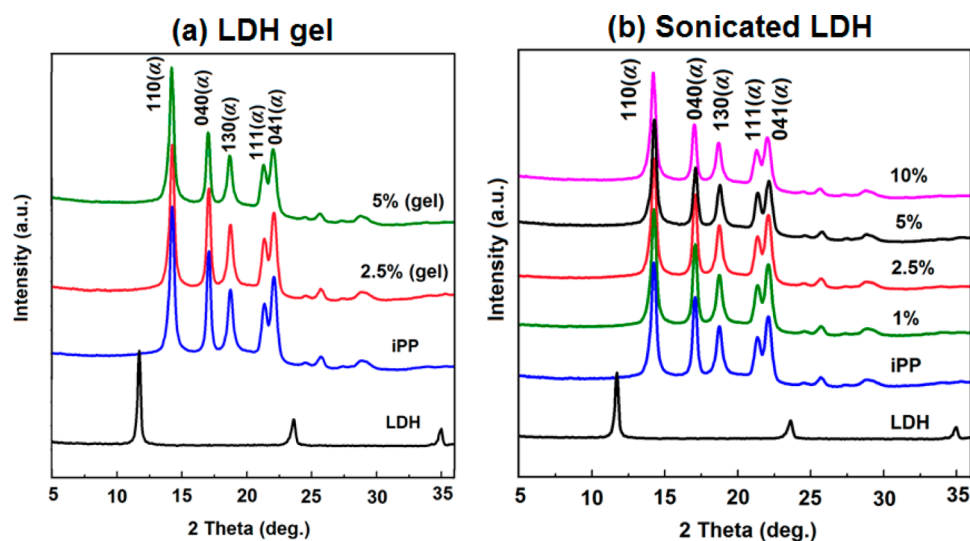
Figure 5. Powder X-ray diffraction data for (a) iPP nanocomposites prepared by using LDH gel and (b) iPP nanocomposites prepared by using sonicated LDH. For the purpose of comparison, powder X-ray diffraction data iPP and LDH are shown in both a and b.

dispersed to single-layer nanosheets in the polymer solution to obtain the highly dispersed nanocomposites. In another method, sonicated Mg−Al LDH (broken LDH fragments) was added to iPP solution to obtain highly dispersed nanocomposites. As mentioned in the preceding section, replacement of water molecules with organic solvents weakens the interaction between the Mg−Al LDH platelets, which helps in delamination of these platelets when dispersed in iPP solution. The resultant solution was poured into ethanol. The precipitate was filtered, washed with excess ethanol and dried under vacuum overnight. In order to compare the properties of iPP and iPP/LDH nanocomposites under the similar conditions, pristine iPP powder was also prepared under similar treatment.

Figure 5 shows the X-ray diffraction patterns of Mg−Al LDH, iPP and its nanocomposites containing different amounts of LDH. Unlike other reported iPP/LDH nanocomposites, the reflections corresponding to the (00n) planes of LDH are not

observed in both the nanocomposites (prepared using LDH gel and sonicated LDH).[18,48] Such disappearance of LDH reflections is due to the loss of periodicity of the LDH. These results suggest that Mg−Al LDH platelets are exfoliated and well dispersed in the polymer matrix. iPP and nanocomposites are crystallized isothermally at 130 °C after melting at 200 °C under strictly controlled conditions to understand the influence of LDH on polymorphic behavior of iPP. Both iPP and iPP/LDH nanocomposites show reflections at 2θ = 14.2°, 17.0°, 18.7°, 21.3°, and 22.1° corresponding to the monoclinic α form of iPP.[49] No change in the polymorphism of iPP was observed in the presence of LDH platelets. Table 1 shows the degree of crystallinity of iPP matrix in the iPP/LDH nanocomposites. The degree of crystallinity was calculated as the ratio of the area under the crystalline peaks to the total area under the X-ray scattering curve. It can be clearly seen that the nanocomposites prepared using LDH gel showed less crystallinity (~57%) compared to the nanocomposites

Table 1. Degree of Crystallinity and 50% Weight Loss Temperature of iPP and its Nanocomposites after Melt Crystallization at 130 °C

sample	% crystallinity WAXS (± 0.5)	50% weight loss temperature (°C) (± 1)
iPP	65	411
iPP−LDH gel (2.5%)	59	434
iPP−LDH gel (5%)	57	431
iPP−sonicated LDH (1%)	65	448
iPP−sonicated LDH (2.5%)	64	439
iPP−sonicated LDH (5%)	63	433
iPP−sonicated LDH (10%)	66	430

prepared using sonicated LDH (∼65%). The low crystallinity of the nanocomposites using LDH gel is due to the fact that the crystalline lamellar growth of iPP might be hindered to some extent in the presence of larger LDH particles having lateral size 2−3 μm.

The dispersion of LDH particles in iPP matrix was further confirmed by AFM measurements. Nanocomposite thin film was prepared by melt pressing the powder samples in between the coverslips. Figure 6 shows the AFM phase images of 10 wt
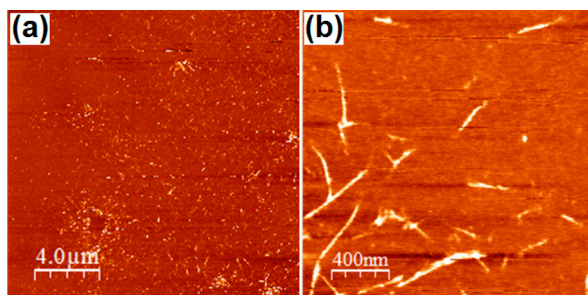

Figure 6. AFM images of iPP nanocomposite film containing 10 wt % of sonicated LDH (a) 20 μm × 20 μm (b) 2 μm × 2 μm.

% of sonicated LDH containing nanocomposite film. It is obvious from the figure that nanosized LDH platelets with a few nanometers thickness and few hundreds of nm length are homogeneously dispersed in the iPP matrix. It is worth mentioning here that the breadth of the nanoparticles/nanodots appears much larger in the AFM image than the true values due to the AFM tip surface convolution effect.[50,51]

The influence of nanocomposites preparation method and various loadings of LDH on the thermal stability of iPP were investigated by TGA under nitrogen atmosphere. The corresponding TGA thermograms are shown in Figure 7. The 50% weight loss temperature ($T_{0.5}$) measured for various samples are summarized in Table 1. All the nanocomposite samples showed higher thermal stability than that of the pure iPP. Nanocomposites prepared using the gel form of LDH showed lower thermal stability than that of the nanocomposites prepared using same weight percent of sonicated LDH. However, significant differences are seen in thermal stability of nanocomposites prepared using different weight percent of sonicated LDH. The nanocomposite prepared with 1 wt % of sonicated LDH showed better thermal stability than the other nanocomposites. The $T_{0.5}$ increases from 411 °C for pure iPP to 448 °C with 1 wt % of sonicated LDH, and then gradually decreased to 430 °C (10 wt % of sonicated LDH) with the increase in weight percent of sonicated LDH loadings. O'Hare and co-workers reported 9 wt % LDH as optimal loading for the nanocomposites prepared using acetone washed LDH.[18] In another study, the same group showed higher thermal stability for iPP at 1 wt % LDH loadings in surfactant-modified Mg−Al LDH/PP nanocomposites synthesized by microemulsion method.[17] Based on the results obtained in this paper for the LDH gel samples and the literature data, we are speculating here that the radicals generated during degradation were trapped by the well dispersed LDH nanoparticles.[17,18] Lower loadings of sonicated LDH might be dispersed well in iPP matrix compared to excessive loadings and probably is the reason why $T_{0.5}$ is higher for lower LDH loadings in nanocomposites prepared using sonicated LDH. It is also worth mentioning here that the nanocomposites prepared using gel form of LDH has less number of dispersed particles compare to that of nanocomposites prepared by sonicated LDH with equivalent amounts of LDH loadings. It might be the reason for lower thermal stability of nanocomposites containing gel form of LDH compared to that of nano-composites with sonicated LDH.
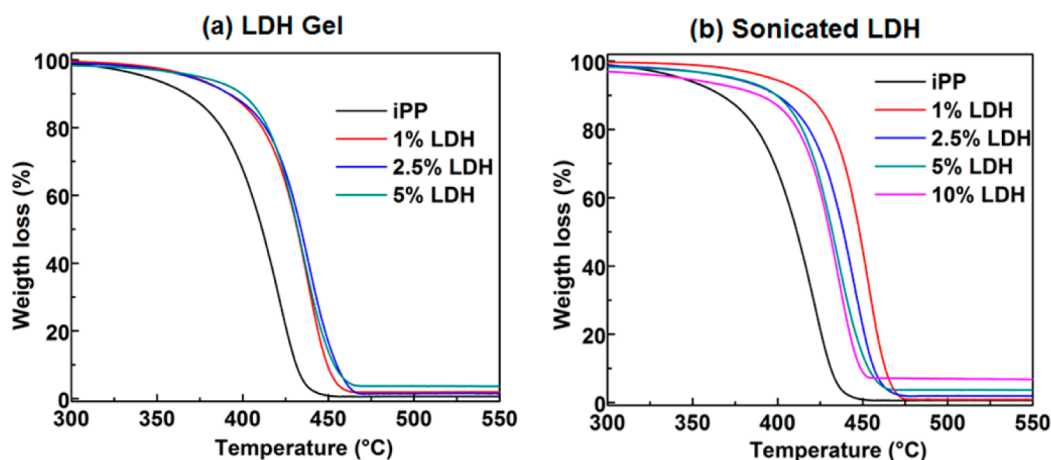
Figure 7. TGA thermograms for (a) iPP nanocomposites prepared by using LDH gel (0, 2.5, and 5% loadings) and (b) iPP nanocomposites prepared by using sonicated LDH (0, 1, 2.5, 5, and 10% loadings).

**Crystallization Behavior of iPP/Mg–Al LDH Nano-composites.** Figure 8 shows the POM images of iPP and its
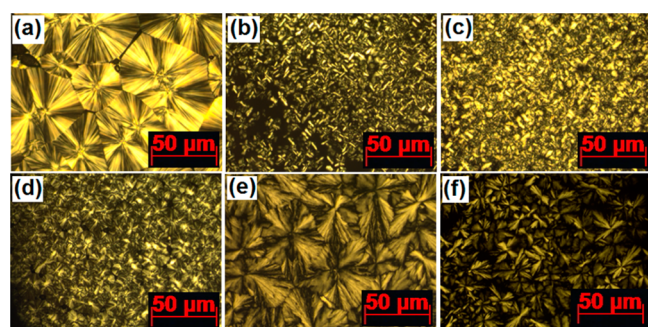
Figure 8. Polarized optical micrographs of pure iPP and its nanocomposites crystallized isothermally at 130 °C: (a) iPP, (b) iPP/1 wt % sonicated LDH, (c) iPP/5 wt % sonicated LDH, (d) iPP/10 wt % sonicated LDH, (e) iPP/2.5 wt % of LDH gel, and (f) iPP/5 wt % of LDH gel.

nanocomposites prepared using both sonicated LDH and gel form of LDH after isothermal crystallization at 130 °C. Under the given conditions (samples melted at 200 °C for 3 min then rapidly cooled to isothermal crystallization temperature 130 °C for 30 min), pure iPP crystallized into larger spherulites with an average diameter of ~40 μm. Due to the slow crystallization rate, these spherulites grow slowly and collide with each other (Figure 8a). Upon the addition of sonicated LDH, the nucleation density increased and the diameter of the spherulites reduced significantly (Figure 8b–d and Table S1). The uniform size of the spherulites in iPP/LDH nanocomposites (1 wt % sonicated LDH) suggest that highly dispersed LDH platelets act as nucleation sites and barricade iPP spherulite growth. On further increasing the sonicated LDH loadings, the diffuse Maltese cross patterns were observed. On the other hand, when the gel form of LDH was used, the spherulites are imperfect, and the sizes are slightly smaller than that of pure iPP (Figure 8e and f and Table S1). The texture of these spherulites is different from that of the pure iPP. The presence of larger LDH particles hinders the polymer chain diffusion and resulted in imperfect spherulites. It is also worth mentioning here that the nanocomposites prepared with the gel form of LDH showed lower crystallinity compared to that of pure iPP or other

nanocomposites. It was also observed that the size of the spherulites decreased with the increase in LDH content in nanocomposites prepared using the gel form of LDH. By comparing the effect of preparation method of nanocomposites on the crystalline morphology of iPP, it is apparent that the sonicated LDH method provides the largest number of nuclei due to the better dispersion of LDH platelets in iPP matrix.

The effect of LDH on the isothermal melt crystallization kinetics of iPP was studied using DSC. Figure 9 shows the DSC thermograms of pure iPP and its nanocomposites crystallized at 130 °C. The relative crystallinity (X_t) at a given crystallization time was calculated from the DSC exotherms and the plots of X_t against crystallization time for all the samples are shown in Figure 10. It is obvious that all these curves exhibit a sigmoid dependence on time. The crystallization half-time ($t_{1/2}$), which is defined as a half period from the onset of crystallization to the end of crystallization, measured for various samples are summarized in Table 2. The crystallization half-time of pure iPP was 15.9 min. When the LDH was introduced into iPP, the crystallization half-time was decreased for all the nano-composites irrespective of the preparation method. Both the induction time and the width of the exotherm decreased, reflecting an enhancement in the crystallization rate of iPP in the presence of LDH particles. However, significant differences have been observed in the crystallization rate of nano-composites prepared by different methods. When the gel form of LDH was added into iPP, the crystallization half-time decreased moderately with the increase of LDH content. On the other hand, when the sonicated LDH was added into iPP, the crystallization rate was greatly enhanced, demonstrating the high nucleation ability of sonicated LDH particles. As the sonicated LDH loadings increase, the crystallization half-time first decreases from 15.9 min for pure iPP to 2.0 min with 2.5 wt % of sonicated LDH. Further increase in the LDH content, the crystallization half-time was increased to 3.9 min with 10 wt % of sonicated LDH. These results suggested that 2.5 wt % of sonicated LDH is the optimal loading for the effective crystallization of iPP due to its better dispersion in iPP matrix. As observed in the AFM image shown in Figure 6, higher loadings of LDH shows some agglomerates and it might be responsible for the slower crystallization of iPP with higher loadings. The better nucleation ability of iPP in the presence of sonicated LDH might be due to the high surface area of broken
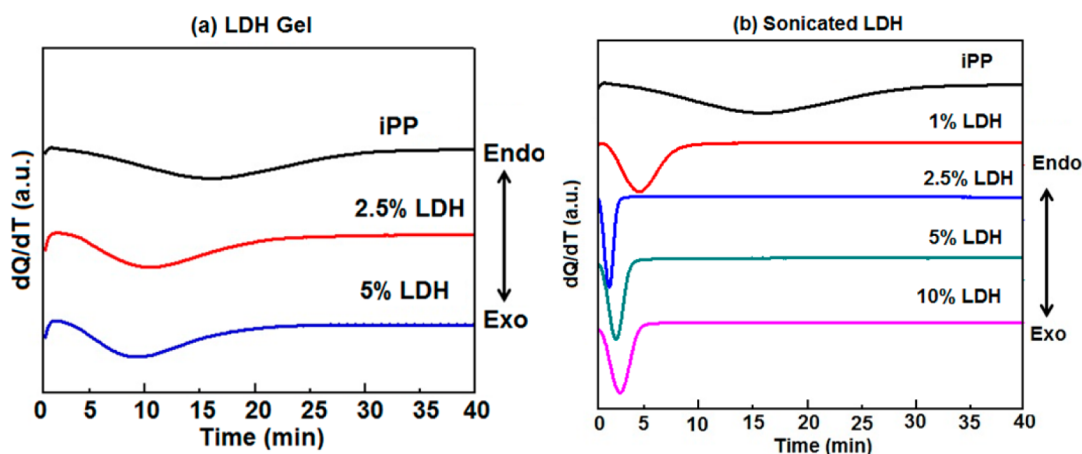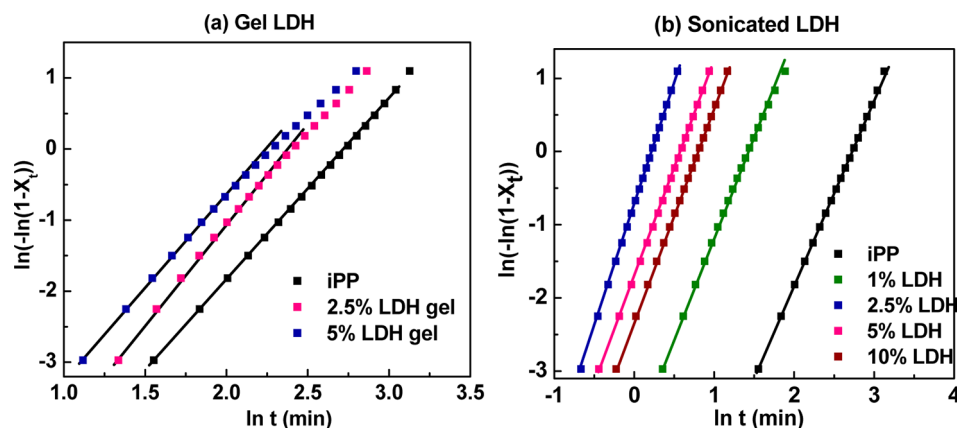

Figure 9. Crystallization isotherms obtained at 130 °C for pure iPP and its nanocomposites. (a) iPP nanocomposites using LDH gel (0, 2.5, and 5% loadings) and (b) iPP nanocomposites using sonicated LDH (0, 1, 2.5, 5, and 10% loadings). The curves were shifted vertically for legibility.
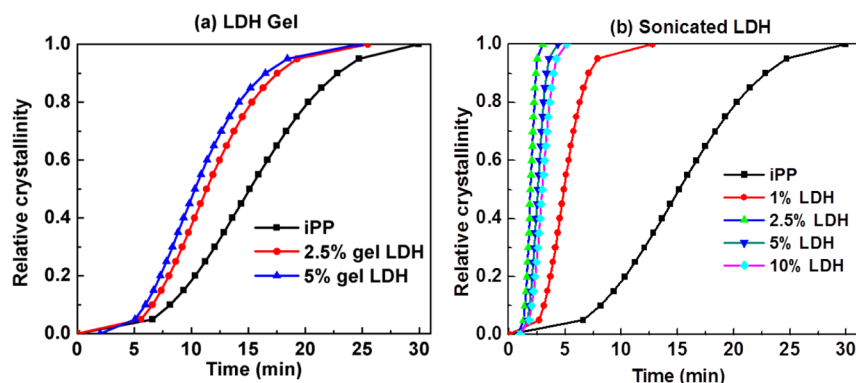
Figure 10. Variation in relative crystallinity with crystallization time for pure iPP and its nanocomposites crystallized isothermally at 130 °C. (a) iPP nanocomposites using LDH gel (0, 2.5, and 5% loadings) and (b) iPP nanocomposites using sonicated LDH (0, 1, 2.5, 5, and 10% loadings).

Table 2. Crystallization Half-Time, Melt Crystallization Temperature, Melting Temperature, and Avrami Constant of iPP and Its Nanocomposites

sample	crystallization half-time (min) at 130 °C (± 0.2)	melt crystallization temperature (T_{mc}) °C (± 0.3)	melting temperature (T_m) °C (± 0.5)	Avrami constant n (± 0.05)
iPP	15.9	109	165.1	2.6
iPP−LDH gel (2.5%)	10.3	112.7	151.4	2.6
iPP−LDH gel (5%)	9.3	116	151.4	2.5
iPP−sonicated LDH (1%)	4.7	118.0	158.7	2.8
iPP−sonicated LDH (2.5%)	2.0	123	163.8	3.4
iPP−sonicated LDH (5%)	2.7	121.1	160.7	3.0
iPP−sonicated LDH (10%)	3.9	119.8	163.5	2.9

Figure 11. Plots of $\ln[-\ln(1 - X_t)]$ versus $\ln(t)$ for pure iPP and its nanocomposites crystallized isothermally at 130 °C. (a) iPP nanocomposites using LDH gel (0, 2.5, and 5% loadings) and (b) iPP nanocomposites using sonicated LDH (0, 1, 2.5, 5, and 10% loadings).

LDH platelets along with its better dispersibility within the polymer matrix.

Isothermal crystallization kinetics for pure iPP and its nanocomposites were analyzed using Avrami equation according to the dependence of X_t on the crystallization time (t).[52,53]

$$1 - X(t) = \exp(-Kt^n) \qquad (1)$$

Where $X(t)$ is the relative crystallinity, n is the Avrami exponent (which is dependent on the nature of nucleation and crystal growth geometry), and K is the overall isothermal crystallization rate constant connected with both nucleation and crystal growth contributions. The linear form of eq 1 can be expressed by taking a logarithmic transformation:

$$\ln[-\ln(1 - X_t)] = \ln K + n \ln(t) \qquad (2)$$

By plotting $\ln[-\ln(1 - X_t)]$ versus $\ln(t)$, the Avrami parameters (n and K) may be directly obtained from the slope and the intercept, respectively, from the early linear segment. Figure 11 shows such plots for pure iPP and its nanocomposites prepared by using LDH gel and sonicated LDH. Table 2 summarizes the Avrami constants estimated for various samples crystallized at 130 °C. The n value of pure iPP was ∼2.6, which was comparable to the literature values.[54,55] This n value might be attributed to a heterogeneous nucleation followed by diffusion controlled spherulite growth (mixed two-dimensional (2D) and three-dimensional (3D) crystal growth). The nanocomposites prepared using the gel form of LDH
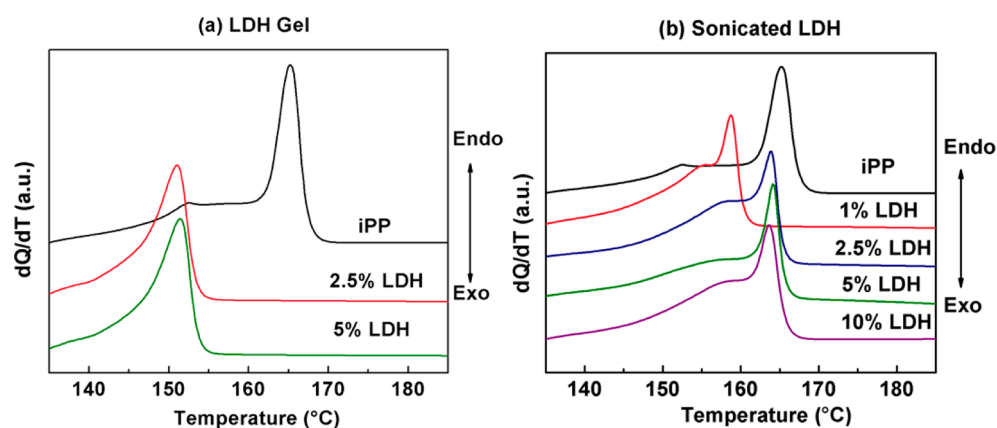
Figure 12. DSC melting thermograms for pure iPP and its nanocomposites crystallized isothermally at 130 °C. (a) iPP nanocomposites using LDH gel (0, 2.5, and 5% loadings) and (b) iPP nanocomposites using sonicated LDH (0, 1, 2.5, 5, and 10% loadings). The curves were shifted vertically for legibility.
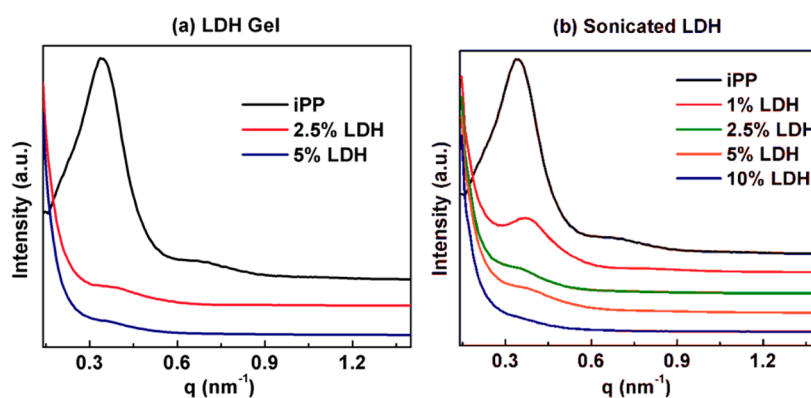
Figure 13. Small-angle X-ray scattering profiles of pure iPP and its nanocomposites crystallized isothermally at 130 °C. (a) iPP nanocomposites using LDH gel (0, 2.5, and 5% loadings) and (b) iPP nanocomposites using sonicated LDH (0, 1, 2.5, 5, and 10% loadings).

showed n value similar to the pure iPP suggesting that the delaminated LDH platelets did not change the crystallization mechanism of iPP. On the other hand, the n value fluctuates within the range of 2.8−3.4 for the nanocomposites prepared using sonicated LDH, also indicating the same crystallization mechanism. The n value around three is typical for a rapidly nucleating system undergoing 3D crystal growth. The DSC results discussed here are very much consistent with iPP spherulitic morphology, which is shown in Figure 8.

First DSC cooling thermograms from the melt of the corresponding samples are shown in Figure S4. The melt crystallization temperature (T_{mc}) is often used to measure the crystallization rate of semicrystalline polymers. Table 2 summarizes the T_{mc} values obtained for iPP and various nanocomposites. Figure S5 shows a plot of crystallization half-time versus T_{mc}. The linear behavior shows the consistency in the crystallization rate of iPP and its nanocomposites by isothermal and nonisothermal crystallization methods. Similar conclusions as those made in the preceding section may be drawn about the effect of LDH on the crystallization rate of iPP.

Melting Behavior of iPP/Mg−Al LDH Nanocomposites. The influence of LDH particles size and concentration on the melting behavior of iPP were studied by heating the isothermally crystallized iPP samples at a heating rate of 10 °C/min. Figure 12 shows the melting thermograms of iPP and its nanocomposites containing different sized LDH particles

(prepared by using the gel form of LDH and sonicated LDH). Clearly, the size of LDH has a dramatic impact on the melting behavior of iPP. The melting temperatures of various samples are summarized in Table 2. Pure iPP shows double melting behavior with a dominant peak at 165.1 °C. X-ray diffractograms obtained for these samples ruled out the possibility of different crystalline polymorph, which is not the reason for double melting behavior in this situation. As already pointed out in literature, double melting peaks are the result of partial melting followed by recrystallization during heating. It means in pristine iPP, the shoulder peak might corresponds to the melting of crystals that formed at isothermal crystallization temperature (130 °C) and upon heating the sample recrystallized and melted at high melting temperature peak (165.1 °C). With the addition of larger sized particles (prepared using the gel form of LDH), the melting temperature of iPP decreased drastically to 151.4 °C. In these samples, high melting temperature peak was absent due to the presence of larger LDH particles. These larger particles hinder the polymer chain diffusion and recrystallization during heating. As a result a single large endotherm was observed in nanocomposites prepared using the gel form of LDH. On the other hand, the nanocomposites prepared using the sonicated LDH showed melting behavior similar to that of pure iPP. These results confirmed that the lateral size of the LDH particles play an important role in controlling the recrystallization of polymer chains during heating. All the nanocomposite samples

containing sonicated LDH particles showed double melting peaks as a result of partial melting followed by recrystallization during heating. The shoulder peak presented at lower temperature for pure iPP shifts to the higher temperature upon the addition of sonicated LDH particles, which might be due to the changes in crystallite thickness and its distribution. In this way, it was found that the size of LDH and its dispersion in the polymer matrix can significantly affect the melting behavior of iPP.

The SAXS intensities for both pure iPP and the nanocomposites prepared by using the gel form of LDH and sonicated LDH are shown in Figures 13. Pure iPP sample shows first maxima (q_1) at $(0.37 \ \text{nm}^{-1})$ attributed to the alternating crystalline and amorphous microstructure of the lamellae. Additional scattering peaks are seen for pure iPP at higher q indicating the regular stacking of lamellar structures. The integer ratio between the scattering peaks is characteristic of a periodic lamellar structure.[36,56] On the other hand, nanocomposite samples show a weak peak in the q range $(0.35-0.45 \ \text{nm}^{-1})$ corresponding to the iPP lamellar morphology. As discussed in the preceding section, the nanocomposites have comparable levels of degree of crystallinity, but the contrast of the SAXS peak is weak for nanocomposites. It should be noted here that the SAXS measurements were performed in the transmission geometry and some of the X-ray radiation was absorbed by highly dispersed LDH particles in nanocomposites. It is also obvious from Figure 13 that the intensity of the SAXS peak was further reduced with the increase in LDH loadings. Another noteworthy change is the strong scattering intensity at low q in nanocomposites, which can be attributed to the scattering of well-dispersed LDH particles within the iPP matrix.

CONCLUSIONS

In this work, highly dispersed isotactic polypropylene (iPP) nanocomposites having different sized Mg−Al LDH nanoparticles were synthesized using the modified solvent mixing method. The sonication of LDH in xylene enables the modification of LDH surfaces to hydrophobic and simultaneously the LDH layers are broken into small fragments. The dispersion of LDH nanoparticles within the iPP matrix was confirmed by WAXD and atomic force microscopy, which is an indicative of compatibility of LDH nanoparticles with the iPP matrix. We have found that sonicated LDH nanoparticles dramatically improves the thermal stability, nucleation ability, and crystallization rate of iPP at very low LDH loadings compared to that of nanocomposites with larger LDH particles with the same concentration. This might be due to the high surface area of smaller LDH nanoparticles and their better dispersibility within the polymer matrix. The incorporation of LDH nanoparticles did not change the crystallization growth mechanism and crystal structure of iPP.

ASSOCIATED CONTENT

Ⓢ Supporting Information

Figure S1: (a) Surfactant free Mg Al LDH powder, (b) LDH gel formed in xylene. Figure S2: DSC temperature program used for the isothermal crystallization of iPP and its nanocomposites. Figure S3: FTIR spectrum of as-prepared Mg Al LDH sample. Figure S4: DSC cooling thermograms of iPP and its nanocomposites crystallized nonisothermally after melting at temperature 200 °C for 2 min. (a) iPP nanocomposites using LDH gel (0, 2.5, and 5% loadings) and (b)

iPP nanocomposites using sonicated LDH (0, 1, 2.5, 5, and 10% loadings). Figure S5: Crystallization half-time versus melt crystallization temperature. Table S1: Average number of spherulites counted in a given area and average diameter of the spherulites calculated for pristine iPP and its nanocomposites. This material is available free of charge via the Internet at http://pubs.acs.org.

AUTHOR INFORMATION

Corresponding Author
*E-mail: bhojegowd@niist.res.in. Tel.: +91-471-2515474. Fax: +91-471-2491712.

Notes
The authors declare no competing financial interest.

ACKNOWLEDGMENTS

DEDICATION

[†]Dedicated to Prof. Manfred Stamm on the occasion of his 65th birthday.

REFERENCES

(1) Wang, Q.; O'Hare, D. Recent Advances in the Synthesis and Application of Layered Double Hydroxide (LDH) Nanosheets. *Chem. Rev.* **2012**, *112*, 4124−4155.

(2) Sinha Ray, S.; Okamoto, M. Polymer/Layered Silicate Nanocomposites: A Review from Preparation to Processing. *Prog. Polym. Sci.* **2003**, *28*, 1539−1641.

(3) Kim, H.; Abdala, A. A.; Macosko, C. W. Graphene/Polymer Nanocomposites. *Macromolecules* **2010**, *43*, 6515−6530.

(4) Leroux, F.; Adachi-Pagano, M.; Intissar, M.; Chauviere, S.; Forano, C.; Besse, J.-P. Delamination and Restacking of Layered Double Hydroxides. *J. Mater. Chem.* **2001**, *11*, 105−112.

(5) Basu, D.; Das, A.; Stöckelhuber, K. W.; Wagenknecht, U.; Heinrich, G. Advances in Layered Double Hydroxide (LDH)-Based Elastomer Composites. *Prog. Polym. Sci.* **2014**, *39*, 594−626.

(6) Vaia, R. A.; Giannelis, E. P. Polymer Nanocomposites: Status and Opportunities. *MRS Bull.* **2001**, *26*, 394−401.

(7) Fu, X.; Qutubuddin, S. Polymer−Clay Nanocomposites: Exfoliation of Organophilic Montmorillonite Nanolayers in Polystyrene. *Polymer* **2001**, *42*, 807−813.

(8) Leroux, F.; Besse, J.-P. Polymer Interleaved Layered Double Hydroxide: A New Emerging Class of Nanocomposites. *Chem. Mater.* **2001**, *13*, 3507−3515.

(9) Costa, F.; Saphiannikova, M.; Wagenknecht, U.; Heinrich, G., Layered Double Hydroxide Based Polymer Nanocomposites. In *Wax Crystal Control · Nanocomposites · Stimuli-Responsive Polymers*; Springer: Berlin Heidelberg, 2008; Chapter 123, pp 101−168.

(10) Meyn, M.; Beneke, K.; Lagaly, G. Anion-Exchange Reactions of Layered Double Hydroxides. *Inorg. Chem.* **1990**, *29*, 5201−5207.

(11) Borja, M.; Dutta, P. K. Fatty Acids in Layered Metal Hydroxides: Membrane-Like Structure and Dynamics. *J. Phys. Chem.* **1992**, *96*, 5434−5444.

(12) Zhao, Y.; Li, F.; Zhang, R.; Evans, D. G.; Duan, X. Preparation of Layered Double-Hydroxide Nanomaterials with a Uniform Crystallite Size Using a New Method Involving Separate Nucleation and Aging Steps. *Chem. Mater.* **2002**, *14*, 4286−4291.

(13) Ogawa, M.; Kaiho, H. Homogeneous Precipitation of Uniform Hydrotalcite Particles. *Langmuir* **2002**, *18*, 4240−4242.

(14) Chen, W.; Qu, B. Structural Characteristics and Thermal Properties of PE-g-MA/MgAl-LDH Exfoliation Nanocomposites Synthesized by Solution Intercalation. *Chem. Mater.* **2003**, *15*, 3208−3213.

(15) Chen, W.; Feng, L.; Qu, B. Preparation of Nanocomposites by Exfoliation of ZnAl Layered Double Hydroxides in Nonpolar LLDPE Solution. *Chem. Mater.* **2004**, *16*, 368−370.

(16) Chen, W.; Qu, B. LLDPE/ZnAl LDH-Exfoliated Nano-composites: Effects of Nanolayers on Thermal and Mechanical Properties. *J. Mater. Chem.* **2004**, *14*, 1705−1710.

(17) Wang, Q.; Zhang, X.; Wang, C. J.; Zhu, J.; Guo, Z.; O'Hare, D. Polypropylene/Layered Double Hydroxide Nanocomposites. *J. Mater. Chem.* **2012**, *22*, 19113−19121.

(18) Wang, Q.; Zhang, X.; Zhu, J.; Guo, Z.; O'Hare, D. Preparation of Stable Dispersions of Layered Double Hydroxides (LDHs) in Nonpolar Hydrocarbons: New Routes to Polyolefin/Ldh Nano-composites. *Chem. Commun.* **2012**, *48*, 7450−7452.

(19) Wang, D.-Y.; Das, A.; Costa, F. R.; Leuteritz, A.; Wang, Y.-Z.; Wagenknecht, U.; Heinrich, G. Synthesis of Organo Cobalt−Aluminum Layered Double Hydroxide via a Novel Single-Step Self-Assembling Method and Its Use as Flame Retardant Nanofiller in PP. *Langmuir* **2010**, *26*, 14162−14169.

(20) Lonkar, S. P.; Morlat-Therias, S.; Caperaa, N.; Leroux, F.; Gardette, J. L.; Singh, R. P. Preparation and Nonisothermal Crystallization Behavior of Polypropylene/Layered Double Hydroxide Nanocomposites. *Polymer* **2009**, *50*, 1505−1515.

(21) Zammarano, M.; Bellayer, S.; Gilman, J. W.; Franceschi, M.; Beyer, F. L.; Harris, R. H.; Meriani, S. Delamination of Organo-Modified Layered Double Hydroxides in Polyamide 6 by Melt Processing. *Polymer* **2006**, *47*, 652−662.

(22) Peng, H.; Tjiu, W. C.; Shen, L.; Huang, S.; He, C.; Liu, T. Preparation and Mechanical Properties of Exfoliated CoAl Layered Double Hydroxide (LDH)/Polyamide 6 Nanocomposites by in Situ Polymerization. *Compos. Sci. Technol.* **2009**, *69*, 991−996.

(23) Illaik, A.; Taviot-Guého, C.; Lavis, J.; Commereuc, S.; Verney, V.; Leroux, F. Unusual Polystyrene Nanocomposite Structure Using Emulsifier-Modified Layered Double Hydroxide as Nanofiller. *Chem. Mater.* **2008**, *20*, 4854−4860.

(24) Pan, P.; Zhu, B.; Dong, T.; Inoue, Y. Poly(L-Lactide)/Layered Double Hydroxides Nanocomposites: Preparation and Crystallization Behavior. *J. Polym. Sci., Part B: Polym. Phys.* **2008**, *46*, 2222−2233.

(25) Wang, D.-Y.; Leuteritz, A.; Wang, Y.-Z.; Wagenknecht, U.; Heinrich, G. Preparation and Burning Behaviors of Flame Retarding Biodegradable Poly(Lactic Acid) Nanocomposite Based on Zinc Aluminum Layered Double Hydroxide. *Polym. Degrad. Stab.* **2010**, *95*, 2474−2480.

(26) Manzi-Nshuti, C.; Wang, D.; Hossenlopp, J. M.; Wilkie, C. A. Aluminum-Containing Layered Double Hydroxides: The Thermal, Mechanical, and Fire Properties of (Nano) Composites of Poly-(Methyl Methacrylate). *J. Mater. Chem.* **2008**, *18*, 3091−3102.

(27) Zhu, H.; Wang, W.; Liu, T. Effects of Copper-Containing Layered Double Hydroxide on Thermal and Smoke Behavior of Poly(Vinyl Chloride). *J. Appl. Polym. Sci.* **2011**, *122*, 273−281.

(28) Wang, Q.; Undrell, J. P.; Gao, Y.; Cai, G.; Buffet, J.-C.; Wilkie, C. A.; O'Hare, D. Synthesis of Flame-Retardant Polypropylene/LDH-Borate Nanocomposites. *Macromolecules* **2013**, *46*, 6145−6150.

(29) Song, F.; Hu, X. Exfoliation of Layered Double Hydroxides for Enhanced Oxygen Evolution Catalysis. *Nat. Commun.* **2014**, *5*, No. 4477.

(30) Wang, Q.; O'Hare, D. Large-Scale Synthesis of Highly Dispersed Layered Double Hydroxide Powders Containing Delaminated Single Layer Nanosheets. *Chem. Commun.* **2013**, *49*, 6301−6303.

(31) Yang, M.; McDermott, O.; Buffet, J.-C.; O'Hare, D. Synthesis and Characterisation of Layered Double Hydroxide Dispersions in Organic Solvents. *RSC Adv.* **2014**, *4*, 51676−51682.

(32) Fornes, T. D.; Paul, D. R. Crystallization Behavior of Nylon 6 Nanocomposites. *Polymer* **2003**, *44*, 3945−3961.

(33) Li, L.; Li, C. Y.; Ni, C. Polymer Crystallization-Driven, Periodic Patterning on Carbon Nanotubes. *J. Am. Chem. Soc.* **2006**, *128*, 1692−1699.

(34) Maiti, P.; Nam, P. H.; Okamoto, M.; Hasegawa, N.; Usuki, A. Influence of Crystallization on Intercalation, Morphology, and Mechanical Properties of Polypropylene/Clay Nanocomposites. *Macromolecules* **2002**, *35*, 2042−2049.

(35) Nam, P. H.; Maiti, P.; Okamoto, M.; Kotaka, T.; Hasegawa, N.; Usuki, A. A Hierarchical Structure and Properties of Intercalated Polypropylene/Clay Nanocomposites. *Polymer* **2001**, *42*, 9633−9640.

(36) Liu, P.; White, K. L.; Sugiyama, H.; Xi, J.; Higuchi, T.; Hoshino, T.; Ishige, R.; Jinnai, H.; Takahara, A.; Sue, H.-J. Influence of Trace Amount of Well-Dispersed Carbon Nanotubes on Structural Development and Tensile Properties of Polypropylene. *Macromolecules* **2013**, *46*, 463−473.

(37) Grady, B. P.; Pompeo, F.; Shambaugh, R. L.; Resasco, D. E. Nucleation of Polypropylene Crystallization by Single-Walled Carbon Nanotubes. *J. Phys. Chem. B* **2002**, *106*, 5852−5858.

(38) Xu, J.-Z.; Chen, C.; Wang, Y.; Tang, H.; Li, Z.-M.; Hsiao, B. S. Graphene Nanosheets and Shear Flow Induced Crystallization in Isotactic Polypropylene Nanocomposites. *Macromolecules* **2011**, *44*, 2808−2818.

(39) Lonkar, S. P.; Singh, R. P. Isothermal Crystallization and Melting Behavior of Polypropylene/Layered Double Hydroxide Nanocomposites. *Thermochim. Acta* **2009**, *491*, 63−70.

(40) Liu, Z.; Ma, R.; Osada, M.; Iyi, N.; Ebina, Y.; Takada, K.; Sasaki, T. Synthesis, Anion Exchange, and Delamination of Co−Al Layered Double Hydroxide: Assembly of the Exfoliated Nanosheet/Polyanion Composite Films and Magneto-Optical Studies. *J. Am. Chem. Soc.* **2006**, *128*, 4872−4880.

(41) Costantino, U.; Marmottini, F.; Nocchetti, M.; Vivani, R. New Synthetic Routes to Hydrotalcite-Like Compounds − Characterisation and Properties of the Obtained Materials. *Eur. J. Inorg. Chem.* **1998**, *1998*, 1439−1446.

(42) Nicolosi, V.; Chhowalla, M.; Kanatzidis, M. G.; Strano, M. S.; Coleman, J. N. Liquid Exfoliation of Layered Materials. *Science* **2013**, *340*, No. 1226419.

(43) Coleman, J. N.; Lotya, M.; O'Neill, A.; Bergin, S. D.; King, P. J.; Khan, U.; Young, K.; Gaucher, A.; De, S.; Smith, R. J.; Shvets, I. V.; Arora, S. K.; Stanton, G.; Kim, H.-Y.; Lee, K.; Kim, G. T.; Duesberg, G. S.; Hallam, T.; Boland, J. J.; Wang, J. J.; Donegan, J. F.; Grunlan, J. C.; Moriarty, G.; Shmeliov, A.; Nicholls, R. J.; Perkins, J. M.; Grieveson, E. M.; Theuwissen, K.; McComb, D. W.; Nellist, P. D.; Nicolosi, V. Two-Dimensional Nanosheets Produced by Liquid Exfoliation of Layered Materials. *Science* **2011**, *331*, 568−571.

(44) Wu, Q.; Olafsen, A.; Vistad, O. B.; Roots, J.; Norby, P. Delamination and Restacking of a Layered Double Hydroxide with Nitrate as Counter Anion. *J. Mater. Chem.* **2005**, *15*, 4695−4700.

(45) Han, J. T.; Jang, J. I.; Kim, H.; Hwang, J. Y.; Yoo, H. K.; Woo, J. S.; Choi, S.; Kim, H. Y.; Jeong, H. J.; Jeong, S. Y.; Baeg, K.-J.; Cho, K.; Lee, G.-W. Extremely Efficient Liquid Exfoliation and Dispersion of Layered Materials by Unusual Acoustic Cavitation. *Sci. Rep.* **2014**, *4*.

(46) Chhowalla, M.; Shin, H. S.; Eda, G.; Li, L.-J.; Loh, K. P.; Zhang, H. The Chemistry of Two-Dimensional Layered Transition Metal Dichalcogenide Nanosheets. *Nat. Chem.* **2013**, *5*, 263−275.

(47) Qiu, L.; Chen, W.; Qu, B. Structural Characterisation and Thermal Properties of Exfoliated Polystyrene/ZnAl Layered Double Hydroxide Nanocomposites Prepared Via Solution Intercalation. *Polym. Degrad. Stab.* **2005**, *87*, 433−440.

(48) Gao, Y.; Wu, J.; Zhang, Z.; Jin, R.; Zhang, X.; Yan, X.; Umar, A.; Guo, Z.; Wang, Q. Synthesis of Polypropylene/Mg$_3$Al-X (X = CO$_3$$^{2-}$, NO$_3$$^-$, Cl$^-$, SO$_4$$^{2-}$) LDH Nanocomposites Using a Solvent Mixing Method: Thermal and Melt Rheological Properties. *J. Mater. Chem. A* **2013**, *1*, 9928−9934.

(49) Jones, A. T.; Aizlewood, J. M.; Beckett, D. R. Crystalline Forms of Isotactic Polypropylene. *Makromol. Chem.* **1964**, *75*, 134−158.

(50) Gowd, E. B.; Nandan, B.; Bigall, N. C.; Eychmüller, A.; Formanek, P.; Stamm, M. Hexagonally Ordered Arrays of Metallic Nanodots from Thin Films of Functional Block Copolymers. *Polymer* **2010**, *51*, 2661−2667.

(51) Grabar, K. C.; Brown, K. R.; Keating, C. D.; Stranick, S. J.; Tang, S.-L.; Natan, M. J. Nanoscale Characterization of Gold Colloid Monolayers: A Comparison of Four Techniques. *Anal. Chem.* **1997**, *69*, 471−477.

(52) Avrami, M. Kinetics of Phase Change. I General Theory. *J. Chem. Phys.* **1939**, *7*, 1103−1112.

(53) Avrami, M. Kinetics of Phase Change. II Transformation-Time Relations for Random Distribution of Nuclei. *J. Chem. Phys.* **1940**, *8*, 212−224.

(54) Zhang, Y.-F. Isothermal Crystallization Behaviors of Isotactic Polypropylene Nucleated with the Third Generation Sorbitol Derivative Nucleating Agents. *J. Macromol. Sci. Part B−Phys.* **2008**, *47*, 891−899.

(55) Sandler, J.; Broza, G.; Nolte, M.; Schulte, K.; Lam, Y. M.; Shaffer, M. S. P. Crystallization of Carbon Nanotube and Nanofiber Polypropylene Composites. *J. Macromol. Sci. Part B−Phys.* **2003**, *42*, 479−488.

(56) Chu, B.; Hsiao, B. S. Small-Angle X-ray Scattering of Polymers. *Chem. Rev.* **2001**, *101*, 1727−1762.